Available online at www.sciencedirect.com
SCIENCE DIRECT®
ELSEVIER
Nuclear Instruments and Methods in Physics Research A 519 (2004) 651–658
NUCLEAR INSTRUMENTS & METHODS IN PHYSICS RESEARCH Section A
www.elsevier.com/locate/nima

Neutron measurements by passive methods in the Dubna transmutation assemblies

S. Stoulos[a], M. Fragopoulou[a], M. Manolopoulou[a], A. Sosnin[b], M. Krivopustov[b], W. Westmeier[c], R. Brandt[c], M. Debeauvais[d], M. Zamani[a,*]

[a] *Physics Department, Aristotle University of Thessaloniki, Thessaloniki 54124, Greece*
[b] *Joint Institut for Nuclear Research, 141980 Dubna, Russia*
[c] *Philipps Universität, D-35032 Marburg, Germany*
[d] *Institut de Recherche Subatomique, F-67037 Strasbourg, France*

Received 26 May 2003; accepted 15 October 2003

Abstract

In the general case of neutron measurement by passive detectors, the conversion of direct experimental data to neutron flux results by using (1) a cross-section of the reaction on which the detector is responding or (2) an appropriate calibration of the detector versus neutron energy. For a better estimation of the neutron flux, especially in real neutron fields, the calculation of the effective cross-section in the first case and the calculation of an effective conversion factor from Tracks to Neutrons (TN) in the second case, both corresponding to the neutron energy spectrum, is required. This work is an application on the determination and comparison of neutron fluxes in the experimental transmutation assemblies in Dubna using several types of passive detectors. For the calculation of the effective cross-sections as well as of the effective conversion factor TN for each experimental assembly the neutron energy spectral shape was estimated theoretically by using the high-energy transport code DCM-DEM.

PACS: 25.40.S; 29.25.D; 29.40.Y; 82.80.J

Keywords: Passive detectors; Neutron measurements; Spallation reactions

1. Introduction

Transmutation experiments have taken place in Dubna (Laboratory of High Energies) during the last decade by proton irradiations on extensive Pb and U/Pb targets. Various energies ranging from 0.5 to 7.4 GeV were used [1–4] to produce high neutron fluxes by spallation reactions. In these experiments passive detectors such as Solid State Nuclear Track Detectors (SSNTDs) and activation detectors were used for integrated neutron fluence measurements. The SSNTDs were applied as particle detectors with appropriate moderators and as fission detectors with fissile targets. The advantage of SSNTDs is their good response to high neutron fluxes while they are insensitive to gamma rays, which are significant around spallation sources. The collected experimental data, i.e. the counting track density from the SSNTDs and

*Corresponding author. Tel.: +30-2310-998176.
E-mail address: zamani@physics.auth.gr (M. Zamani).

0168-9002/$ - see front matter
doi:10.1016/j.nima.2003.10.087

gamma spectrum from the activation detectors, need to be converted to neutron flux. In both cases the use of a cross-section of the reaction with which the detector is responding must be applied. The use of a typical cross-section corresponding only to a specific energy induces to a misestimation of the determined neutron flux, especially when the neutron spectrum extends over a wide energy range, as does a spallation neutron spectrum. Thus, in a real neutron field, for the conversion of the detector information to neutron flux it is important to specify the energy range in which each reaction is effective in order to estimate the cross-section which dominates in the spectrum, i.e. an effective cross-section, σ_{eff}. If the above approach is not practiced, large deviations might appear between the results of various detection methods. Therefore to achieve more accurate results (for dosimetry purposes for example) a procedure based on the calculation of an effective cross-section of the reaction with which the detector responds should be applied. Also, an appropriate calibration of the detector readout versus neutron energy could be used. However, the detector response is energy dependent, especially in low energies (thermal-epithermal region), so a similar problem occurs as in the use of the cross-section. For this the calculation of an effective conversion factor from Tracks to Neutrons (TN) corresponding to the neutron energy spectrum is required. For these calculations the neutron energy spectral shape was estimated theoretically by using the high-energy transport code DCM-DEM.

2. Experimental

This work deals with the neutron fluxes produced by spallation sources during two different transmutation experiments performed in Dubna. In the first experiment, the main spallation target, a lead cylinder, was covered with a paraffin moderator, Target (1), and irradiated by 1 GeV proton beam producing a spectrum with a significant thermal and epithermal neutron component [1–4]. In the second experiment, the lead cylinder was covered with a four section U blanket, Target (2), and irradiated by 1.5 GeV proton beam producing mostly intermediate and fast neutrons [5]. Irradiations took place at the Nuclotron accelerator, High Energy Laboratory, JINR, Russia.

Our contribution to these experiments was to determine the neutron flux by using several types of passive detectors i.e. SSNTDs (as particle and fission detectors) and activation detectors (^{238}U, $^{\text{nat}}$Au). A cross-section of the aforementioned experiments is shown in Fig. 1a and b, respectively, wherein the positions of the passive detectors indicated. In this study only the results corresponding on the top and at the middle of the target cover (paraffin or U-blanket) were presented in order to compare the methods.

3. Results and discussion

Cross-sections are energy dependent, so for the conversion of the detector readout to neutron flux it is important to know the energy range in which the cross-section must be considered and then determine the effective cross-section, σ_{eff}. This quantity for a given reaction in an energy interval, E_1-E_2 is calculated by the formula:

$$\sigma_{\text{eff}}(n,x)=\frac{\int_{E_1}^{E_2}\Phi_n(E)\cdot\sigma_{(n,x)}(E)\,\mathrm{d}E}{\int_{E_1}^{E_2}\Phi_n(E)\,\mathrm{d}E}, \tag{1a}$$

where $\Phi_n(E)$ is the energy dependent neutron flux ($\mathrm{n\,cm^{-2}\,MeV^{-1}}$ per proton) and $\sigma_{(n,x)}(E)$ is the energy dependent cross-section. Using exactly the same procedure, the calculation of an effective conversion factor TN for a neutron energy interval, E_1-E_2 following the formula:

$$\mathrm{TN}_{\text{eff}}=\frac{\int_{E_1}^{E_2}\Phi_n(E)\cdot\mathrm{TN}(E)\,\mathrm{d}E}{\int_{E_1}^{E_2}\Phi_n(E)\,\mathrm{d}E} \tag{1b}$$

is required, when the conversion of direct experimental data to neutron flux results by using an appropriate calibration of the detector versus neutron energy.

The other component needed for effective cross-section calculation and for the effective conversion factor calculation is the shape of the energy dependent neutron spectrum, $\Phi(E)$. The neutron spectrum for each experimental setup was theore-

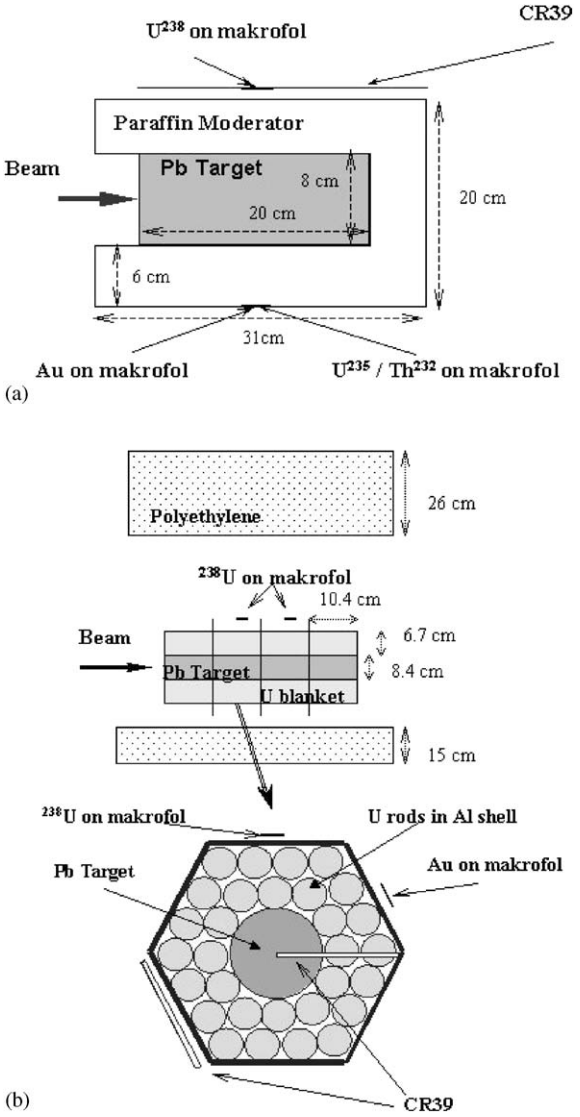

Fig. 1. (a) A cross-section of the Pb(Paraffin) target (1) setup. (b) A cross-section of the Pb(U-blanket) target (2) setup.

tically determined using the high-energy transport code DCM/DEM and is presented in Fig. 2. The DCM/DEM code is a Dubna version of cascade-evaporation approach, similar to Bertini model. This is supplied with high-energy fission and pre-equilibrium evaporation. The calculations correspond to the surface fluxes, i.e. the registered neutrons that cross the unit surface per primary proton. A fitting procedure was applied to the energy dependent neutron flux in order to obtain the necessary value over any energy range [6].

The neutron flux for various energy ranges was determined by using several types of passive detectors as following:

3.1. SSNTDetectors (as particle detectors)

The detecting system includes CR39 detector with $Li_2B_4O_7$ converter (Kodak LR115 Type B) partially covered by 1 mm Cd. An additional CR39 sheet on polyethylene is used [7,8]. In both cases the measured track density N (tracks cm^{-2}) is converted to neutron flux F (neutrons cm^{-2}), according to formula:

$$N = M\sigma_{\text{eff}}F, \tag{2}$$

where M is the number of atoms per cm^2 of the corresponding target and σ_{eff} is the effective cross-section in an energy interval as given by Eq. (1a).

The track density difference between the Cd-covered and uncovered CR39 (plus $Li_2B_4O_7$) detector corresponds to the thermal neutron flux. In particular, considering the cross-section of neutron capture from $^{\text{nat}}$Cd (ENDF/B-VI (300 K) library), 1 mm of Cd induces a neutronically back up to 0.4 eV. For this energy range the cross-sections data given by the ENDF/B-VI (300 K) library for ^{10}B(n,α)^{7}Li reaction were fitted with an $E^{-1/2}$ function and the calculated effective cross-section for both experiments are presented in Table 1.

In addition, the track density on CR39 detectors plus polyethylene originating by proton recoils corresponds to an energy range for intermediate-fast neutrons, $0.3 < E_n < 3$ MeV, due to limitations on registration efficiency of CR39 [9]. In this case, the cross-sections of H(n,n′) elastic scattering were also fitted with an $E^{-1/2}$ function for the energy interval of interest and the calculated effective cross-section for both experiments are presented in Table 2.

Another way to approach the conversion from measured track density N (tracks cm^{-2}) to neutron flux F (neutrons cm^{-2}), is to use an essential conversion factor from Tracks to Neutrons (TN),

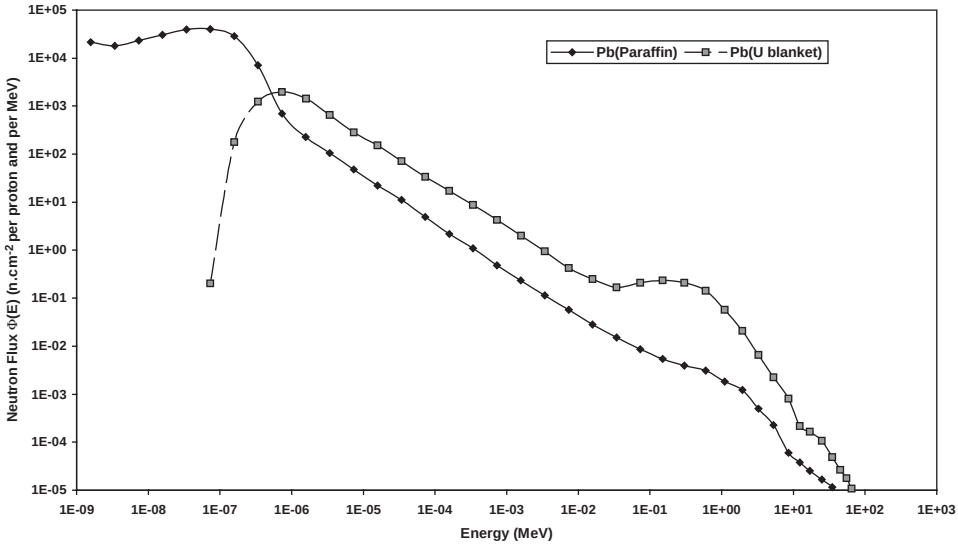

Fig. 2. Theoretical calculation of the neutron flux on the top and at the middle for both experiments using the Dubna Cascade Model (DCM/DEM).

Table 1
The calculated effective conversion factor from tracks to neutrons, TN_{eff}, and σ_{eff} for $^{10}B(n,a)$ reaction with thermal neutron (energy range up to 0.4 eV) for both experiments

Target	Effective conversion factor, TN_{eff}	Effective cross-section, σ_{eff} (b)
(1)	$2.2\ (\pm 0.5) \times 10^{-4}$	2157 ± 378
(2)	$2.2\ (\pm 0.4) \times 10^{-4}$	742 ± 133

Table 2
The calculated effective conversion factor from tracks to neutrons, TN_{eff}, and σ_{eff} for $H(n,n')$ elastic scattering with intermediate-fast neutrons (for energy range $0.3 < E_n < 3$ MeV) for both experiments

Target	Effective conversion factor, TN_{eff}	Effective cross-section, σ_{eff} (b)
(1)	$1.6\ (\pm 0.4) \times 10^{-5}$	4.4 ± 0.9
(2)	$1.2\ (\pm 0.3) \times 10^{-5}$	4.8 ± 0.8

according to formula:

$$N = TN_{eff} F, \tag{3}$$

where TN_{eff} is the effective conversion factor in an energy interval as given by Eq. (1b).

The above conversion factor from Tracks to Neutrons (TN) specifies by the formula:

$$TN(E) = R(E)\, CF(E), \tag{4}$$

where $R(E)$ is the response of the detector to neutron dose (tr cm^{-2} per Gy) and $CF(E)$ is the factor which converts neutron dose to neutron density (Gy per n cm^{-2}). Both components are energy dependent, so the conversion factor from Tracks to Neutrons, $TN(E)$ is also energy dependent and could be determined via an appropriate calibration of the detector response versus neutron energy. Such calibrations have been performed for dosimeter purposes [7,8].

The experimental response, $R(E)$ of the CR39 with $Li_2B_4O_7$ converter [8] and the conversion factor, $CF(E)$ from dose to neutrons [9] as a function of the neutron energy is presented in Fig. 3. Because of the absence of any experimental data in the energy range between thermal to 24 keV neutrons, the response is expressed by a $1/E$ function, as it is presented in Fig. 3 (dash line), considering the conclusions of other specific reports [10,11] where the response has been obtained from Monte Carlo simulations using the MCNP code.

The experimental conversion factor from tracks to neutrons, $TN(E)$ for the CR39 detector with

$Li_2B_4O_7$ converter and polyethylene plus the detector itself (proton recoils) are presented in Fig. 4. In the same figure the calculated conversion factor TN(E) for thermal-epithermal region is also presented. Following a fitting process in both experimental and calculated data, a Two Site Competition function was applied for the CR39 detector with $Li_2B_4O_7$ converter and a Hill function for polyethylene plus CR39 detector (with r^2 coefficient of the fitted parameters 97% and 89%, respectively). The effective conversion factors TN_{eff} for both experiments obtained by the Eq. (1b) are presented in Tables 1 and 2, respectively.

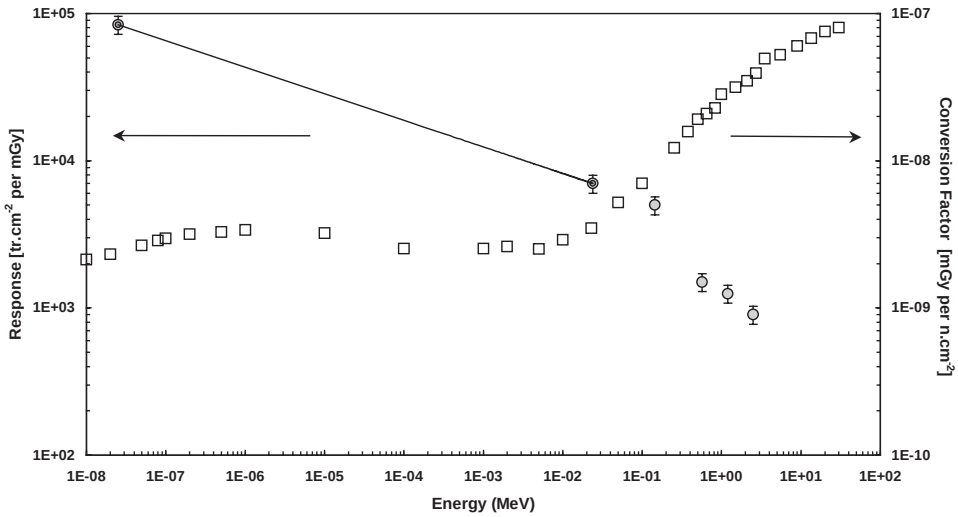

Fig. 3. The experimental response of CR39 with $Li_2B_4O_7$ converter and the conversion factor CF from dose to neutron flux.

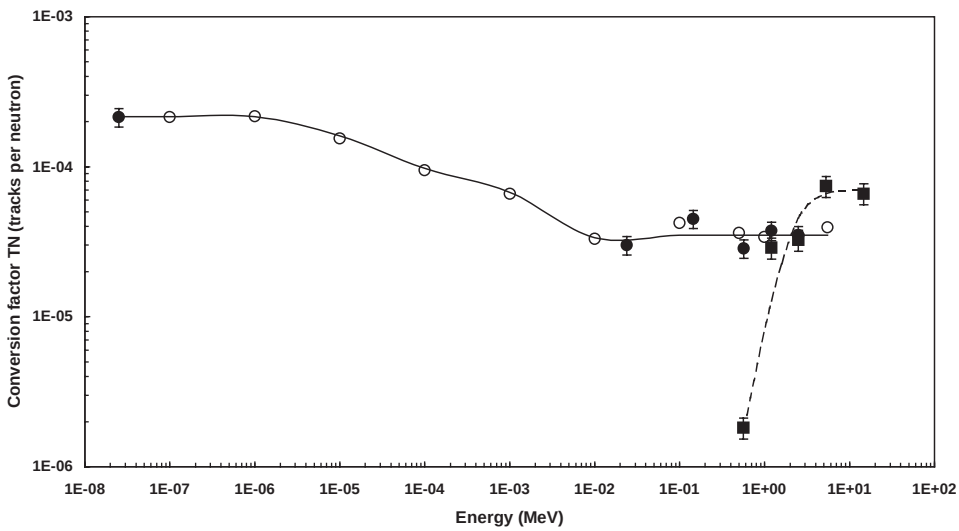

Fig. 4. The conversion factor from tracks to neutrons (TN) for CR39 detector with $Li_2B_4O_7$ converter (○) and polyethylene plus the detector itself (□). The solid symbols represent the experimental data and the dash symbols represent the calculated data. The lines correspond to the fitting process applied in both functions.

3.2. SSNTDetectors (as fission detectors)

Fissile targets of ^{235}U for thermal neutron detection and ^{238}U or ^{232}Th for fast neutron detection were deposited on makrofol by evaporation [12]. After irradiation and appropriate development of the detector, fission track density was counted. The neutron flux was calculated using Eq. (2) with the effective cross-section determined with Eq. (1a). The cross-sections of each reaction are given in Table 3. These values of σ_{eff} are quite different from the commonly used cross-sections as are presented in Table 4, which explains why fission results are always lower than other passive methods. However, the same result is also observed in the application in Dubna transmutation experiments.

3.3. Activation detectors

^{238}U and $^{\text{nat}}$Au activation detector were used for the determination of the epithermal neutron flux using the (n,γ) reaction and fast neutron flux using the (n,2n) reaction. The energy dependent cross-section for ^{238}U and Au (n,γ) as well as for ^{238}U and Au (n,2n) data obtained by the ENDF/B-VI (300 K) library, was fitted with a Gaussian–Lorentzian function on each resonance peak and a Chester-Cram Peak function for (n,2n) reaction (r^2 coefficient of the fitted parameters 96–99%). In the resonance region only those resonance below 200 eV have a strong effect on the calculation of the σ_{eff} [6]. The calculated values of σ_{eff} for both experiments are presented in Table 5.

Table 3
The calculated σ_{eff} for fission detectors

Reaction	Energy range	Effective cross-section, σ_{eff} (b)	
		Target (1)	Target (2)
^{235}U (n,f)	Up to 1 eV	284±80	
^{238}U (n,f)	2–20 MeV	0.72±0.08 (0.66)[a]	0.57±0.04 (0.23)[a]
^{232}Th (n,f)	2–20 MeV	0.21±0.05	0.14±0.03

[a] For the correction of ^{235}U contribution in ^{238}U.

Table 4
Typical cross-sections of some reactions used in neutron detection

Reaction	Cross-section (b)
^{235}U(n,f)	580
^{238}U(n,f)	0.6
^{232}Th(n,f)	0.3

Table 5
The calculated σ_{eff} for activation detectors

Reaction	Energy range	Effective cross-section, σ_{eff} (b)	
		Target (1)	Target (2)
Au (n,γ)	1 eV–10 keV	97±19	194±29
Au (n,2n)	6–20 MeV	1.2±0.1	0.6±0.1
^{238}U (n, γ)	1 eV–10 keV	9±2	29±4
^{238}U (n,2n)	6–20 MeV	1.0±0.1	0.7±0.1

Summarizing, the neutron flux (neutron cm^{-2} per proton) in the Dubna experimental transmutation assemblies corresponding on the top and at the middle of each target cover (paraffin or U-blanket) is presented in Tables 6 and 7, respectively. The comparison between the results obtained by different passive methods shows a good agreement in the same energy range. In the same tables the MC-calculated flux for two major energy ranges, i.e. thermal-epithermal (up to 10 keV) and intermediate-fast (10 keV up to 100 MeV) neutrons, is also presented. The comparison between different experimental methods with the MC calculations, performed by Dubna DCM/DEM high-energy transport code, shows a fair agreement in the thermal-epithermal region, wherein the experimental results extend to the whole corresponding energy range. In the intermediate-fast region the agreement presents to be less good because the experimental results corresponding to slightly different energy regions, extend only to a part of the intermediate-fast neutron range.

4. Conclusion

When passive detectors are used to measure neutron fluxes, large deviations usually appear

Table 6
Neutron flux (neutron cm^{-2} per proton) from 1 GeV proton beam on a thick Pb target with paraffin moderator

Neutron region (energy range)	SSNTDs		Activation detectors	DCM calculated
	Particle detector	Fission detector		
Thermal-Epithermal				$1.3\ (\pm 0.2) \times 10^{-2}$
(Up to 0.4 eV)	$7.4\ (\pm 1.8) \times 10^{-3}$[a] $6.8\ (\pm 1.9) \times 10^{-3}$[b]			
(Up to 1 eV)		$7.7\ (\pm 2.2) \times 10^{-3}$		
(1 eV–10 keV)			$4.8\ (\pm 0.9) \times 10^{-3}$[c] $4.1\ (\pm 0.8) \times 10^{-3}$[d]	
Intermediate-fast				
(0.3–3 MeV)	$7.3\ (\pm 2.2) \times 10^{-3}$[a] $7.6\ (\pm 1.9) \times 10^{-3}$[b]			$1.1\ (\pm 0.1) \times 10^{-2}$
(2–20 MeV)		$1.0\ (\pm 0.3) \times 10^{-3}$		
(6–20 MeV)			$1.6\ (\pm 0.4) \times 10^{-3}$[c] $1.2\ (\pm 0.3) \times 10^{-3}$[d]	

[a] Using Eq. (3).
[b] Using Eq. (2).
[c] ^{238}U reactions.
[d] Au reactions.

Table 7
Neutron flux (neutron cm^{-2} per proton) from 1.5 GeV proton beam on a thick Pb target with U blanket

Neutron Region	SSNTDs		Activation detectors	DCM calculated
(Energy range)	Particle detector	Fission detector		
Thermal-epithermal				$2.8\ (\pm 0.3) \times 10^{-3}$
(Up to 0.4 eV)	$< 2.2 \times 10^{-3}$[a] $< 2.4 \times 10^{-3}$[b]			
(Up to 1 eV)		$1.8\ (\pm 0.6) \times 10^{-3}$		
(1 eV–10 keV)			$1.7\ (\pm 0.4) \times 10^{-3}$[c] $2.1\ (\pm 0.4) \times 10^{-3}$[d]	
Intermediate-fast (0.3–3 MeV)	$4.9\ (\pm 1.6) \times 10^{-2}$[a] $4.4\ (\pm 0.9) \times 10^{-2}$[b]			$1.2\ (\pm 0.1) \times 10^{-1}$
(2–20 MeV)		$9.5\ (\pm 1.5) \times 10^{-3}$		
(6–20 MeV)			$1.6\ (\pm 0.1) \times 10^{-3}$[c] $1.3\ (\pm 0.2) \times 10^{-3}$[d]	

[a] Using Eq. (3)
[b] Using Eq. (2).
[c] ^{238}U reactions.
[d] Au reactions.

between the results obtained by different detection methods. This problem usually is attributed to the different response function of the detectors versus neutron energy. In any energy range the conversion of the detector readout to neutron density needs some conversion factors, which could be the cross-section of the neutron reaction with which the detector responses, or any other conversion factor originating from an appropriate calibration of the detector versus neutron energy. According

to the general principles of detection, the shape of the neutron spectrum plays an important role to the precision of the measurement. So, the foresaid factors are depended upon the energy range as well as the contribution of the neutron spectrum to this specified energy range.

Therefore, to resolve the above problem, it seems to be necessary first to reproduce the neutron spectrum using a Monte Carlo simulation and then to calculate the effective cross-section or the effective conversion factor in any energy region of interest. Following this procedure, a good agreement between results obtained by different passive methods can be achieved for the same energy range. Additional parameters might also be taken into account for each detection system, the most important being the angular response of the detector.

References

[1] J.C. Adloff, R. Brandt, M. Debauvais, F. Fernandez, M.I. Krivopustov, B.A. Kulakov, A.N. Sosnin, M. Zamani, Rad. Meas. 31 (1999) 31.
[2] J.S. Wan, et al., J. Radioanaly. Nucl. Chem. 247 (2001) 151.
[3] J.S. Wan, et al., Nucl. Instr. and Meth. A 463 (2001) 634.
[4] J. Adam, et al., Radiochim. Acta 90 (2002) 431.
[5] M.I. Krivopustov, et al., Kerntechnik 68 (2003) 48.
[6] S. Stoulos, et al., Appl. Rad. Isotopes 58 (2003) 169.
[7] M. Zamani, E. Savvidis, Rad. Prot. Dos. 63 (1996) 299.
[8] E. Savvidis, M. Zamani, Rad. Prot. Dos. 70 (1997) 83.
[9] J.R. Harvey, R.J. Tanner, W.E. Alberts, D.T. Bartlett, E.K. Piesch, H. Shraube, Rad. Prot. Dos. 77 (1998) 267.
[10] T. Bouassoule, F. Fernandez, M. Marin, M. Tomas, Rad. Prot. Dos. 85 (1999) 39.
[11] M. Luszik-Bhadra, W.G. Alberts, E. Dietz, B.R.L. Siebert, Rad. Prot. Dos. 70 (1997) 97.
[12] G. Remy, J. Ralarosy, R. Stein, M. Debeauvais, J. Tripier, J. Phys. 31 (1970) 27.